Intrinsic conductivity of objects having arbitrary shape and conductivity

E. J. Garboczi [1] and J. F. Douglas [2]
[1] *Building Materials, National Institute of Standards and Technology, Gaithersburg, Maryland 20899*
[2] *Polymers Division, National Institute of Standards and Technology, Gaithersburg, Maryland 20899*
(Received 19 January 1996)

We study the electrical conductivity σ of a dispersion of randomly oriented and positioned particle inclusions having common shape and conductivity σ_p, suspended in an isotropic homogeneous matrix of conductivity σ_0. For this problem, the mixture conductivity is a scalar and we concentrate on the leading order concentration virial coefficient, the ''intrinsic conductivity'' $[\sigma]$. Results for $[\sigma]$ are summarized for limiting cases where there is a large mismatch between the conductivities of the inclusions and the suspending matrix. For a general particle shape, we then treat the more difficult case of arbitrary relative conductivity $\Delta \equiv \sigma_p/\sigma_0$ through the introduction of a Padé approximant that incorporates (exact or numerical) information for $[\sigma(\Delta)]$ in the $\Delta \to \infty$, $\Delta \to 0^+$, and $\Delta \approx 1$ limits. Comparison of this approximation for $[\sigma(\Delta)]$ to exact and finite element calculations for a variety of particle shapes in two and three dimensions shows excellent agreement over the entire range of Δ. This relation should be useful for inferring particle shape and property information from conductivity measurements on dilute particle dispersions. The leading order concentration virial coefficient for other mixture properties (thermal conductivity, dielectric constant, refractive index, shear modulus, bulk modulus, viscosity, etc.) are equally well described by a similar Padé approximant. [S1063-651X(96)11106-5]

PACS number(s): 61.41.+e, 72.60.+g

I. INTRODUCTION

Small amounts of additives are often quite effective in modifying the properties of materials. The extent of the effect depends on the property involved, particle dispersion, concentration, and shape, and tends to be larger the more unlike the additive material properties are from those of the suspending matrix. In the common situation of low additive volume fraction, ϕ, the effective properties can be developed in a power series in ϕ. The leading order ''virial coefficient,'' corresponding to the linear order concentration correction to the pure medium property, plays an important role in understanding the influence of particle shape and property mismatch on the effective property of the mixture [1]. The low additive concentration regime is also important in the *inverse problem* of inferring particle shape and/or properties from measurements of effective mixture properties over a range of low additive concentrations. This strategy is commonly followed in the polymer science literature to determine polymer molecular architecture [2].

In a previous paper [1], we made an extensive tabulation of the leading order transport property virial coefficients for a wide range of particle shapes, and a large set of material properties (electrical and thermal conductivity, dielectric constant, refractive index, shear viscosity). Almost all of these previous calculations, analytical and numerical, were restricted to the case where the ratio of the additive property to the matrix property either vanished or diverged. Although the property mismatch between the additive and the matrix may be large, the limits considered previously are clearly idealizations in comparison with real systems where the transport property ratio is generally a finite, nonzero value. The present paper develops an approximate description of transport virial coefficients in terms of the relative conductivity Δ, the ratio of the inclusion conductivity to that of the matrix, and limiting values of the transport virial coefficients for large property mismatch.

In Sec. II we review basic results about the conductivity virial expansion for suspensions of highly conducting and insulating particles, which was the subject of our previous paper [1]. A Padé approximant describing the intrinsic conductivity for general particle shapes and Δ is introduced in Sec. III, and then compared to exact and numerical (finite element) calculations of $[\sigma(\Delta)]$. Some approximations for the limiting values of the transport virial coefficient for large property mismatch are discussed in Sec. IV, which remain to be checked in future numerical studies.

II. REVIEW OF CONDUCTIVITY VIRIAL EXPANSION RESULTS

Maxwell [3] first treated the conductivity σ of a particle suspension in which the suspended spherical particles have a different conductivity σ_p than the suspending medium σ_0. He recognized that the change in conductivity reflected the average dipole moment induced by the particles on the suspending medium in response to an applied field. For a dilute suspension of hard spheres the effect is the simple additive sum of the effects caused by the individuals particle dipoles. The effective conductivity σ of the dilute mixture, for the case of hard spheres, then equals

$$\sigma/\sigma_0 = 1 + [3(\Delta-1)/(\Delta+2)]\phi + O(\phi^2), \quad (2.1a)$$

where $\Delta = \sigma_p/\sigma_0$ is the ''relative conductivity,'' and ϕ is the volume fraction of suspended spherical particles. Exact results that go beyond this classic result are limited, however. There are effective medium calculations that attempt to extend the ''virial expansion'' (2.1a) to higher power of ϕ

[4], but only for the case of spherical inclusions. Sangani [5] recently generalized Maxwell's calculation for spherical particles to d dimensions,

$$\frac{\sigma}{\sigma_0}=1+\frac{d(\Delta-1)\phi}{(\Delta+d-1)}+O(\phi^2). \tag{2.1b}$$

Levine and McQuarrie [6] calculated the second order virial coefficient for highly conducting ($\Delta\to\infty$) spheres, while Jefferey [7] treated this quantity for arbitrary Δ.

The virial expansion (2.1a) has been verified experimentally for dilute suspensions of numerous substances. For example, Eq. (2.1a) implies that the leading order virial coefficient for highly conducting spheres equals 3. This value has been observed by Voet for nearly spherical iron particles (diameter $=10\mu m$) in linseed and mineral oils [8], and has also been found for emulsions of salt water in fuel oil and mercury drops in different oils [9]. The corresponding prediction for insulating suspended spheres, $-\frac{3}{2}$ ($\Delta\to 0$), has been observed for suspensions of glass beads and sand particles in salt solutions [10], and for gas bubbles in salt solutions [11]. Good agreement with Eq. (2.1a) has also been observed in fluidized beds, where the relative conductivity Δ was tuned over a range of values [12].

The practically important inverse problem of determining the volume fraction of a suspension of complicated shaped particles from electrical measurements motivated the generalization of Eq. (2.1a) to particles having arbitrary shape and conductivity. Fricke [13] treated the case of ellipsoidal particles and utilized a Clausius-Mosotti-style [14] effective medium theory to approximate the higher concentration regime. These effective medium calculations are exact in the dilute regime where they reduce to a virial expansion of the form (2.1a). We avoid further discussion of the higher concentration regime where approximate methods must be employed.

The low concentration σ virial expansion of randomly oriented and arbitrarily shaped particles equals [1,15]:

$$\sigma/\sigma_0=1+[\sigma(\Delta)]\phi+O(\phi^2), \tag{2.2a}$$

$$[\sigma(\Delta)]\equiv\lim_{\phi\to 0}(\sigma-\sigma_0)/(\sigma_0\phi), \tag{2.2b}$$

where $[\sigma(\Delta)]$ is called the intrinsic conductivity. We adopt this notation by analogy with the leading order concentration virial for the suspension viscosity which is conventionally called the ''intrinsic viscosity'' $[\eta]$ [2]. The magnitude of $[\sigma(\Delta)]$ can be a strong function of particle shape for extended or flat particles, depending on the magnitude of the relative conductivity Δ, so that the effect of adding a given amount of material to a suspension can be greatly dependent on particle shape.

The polarizability α is a second rank tensor [16,17] that generally depends on particle orientation, shape, size, and Δ. The average polarizability, which is $1/d$ times the trace of the polarizability tensor, is an invariant under rotations [18,19], so that the virial coefficient $[\sigma]=\langle\alpha\rangle/V_p$ is a functional of particle shape and Δ only. Calculation of the average polarizability is often easier than the full polarizability tensor, since any three orthogonal directions can be chosen for the field directions in the calculation of $[\sigma]$. Equivalently, we can angularly average the polarization tensor over all orientation angles with uniform probability [18,19]. In some applications it is useful to orient the suspended particles, in which case the effective conductivity σ of the composite is anisotropic and becomes explicitly dependent on the components of the polarizability tensor [20]. Historically, the anisotropic case was found to be very important in the design of microwave lenses and other artificial dielectrics where large scale conducting elements are arrayed in an insulating matrix [21–24]. The anisotropic situation is also encountered in the optical properties of sheared anisotropic particle suspensions [25]. In the present paper, we emphasize the average polarizability $\langle\alpha\rangle$, which is relevant to suspensions in which the particle orientation is completely random.

In an electrostatic context the polarizability describes how the charges of a body of dielectric constant ϵ_p, embedded in a medium having a dielectric constant ϵ_0, are distorted in response to an applied electric field [14,26]. The distorted charge distribution gives rise to a dipolar field that reacts upon the applied field, thereby modifying the net effective field in the proximity of the body. This connection between conductivity and the dielectric constant is natural since Eqs. (2.1) and (2.2) also describe the dielectric constant of suspensions of particles with a relative dielectric constant $\Delta_\epsilon=\epsilon_p/\epsilon_0$. Moreover, these equations also apply to the magnetic permeability, the diffusion coefficient, and the thermal conductivity of dilute suspensions, where the magnetic field, the concentration gradient, and the temperature gradient are the corresponding ''fields'' [27–29].

Although simple in principle, calculations of the polarizability tensor for objects of general shape is a mathematical problem of notorious difficulty. Indeed, the ellipsoid [13,26] is the only shape in $d=3$ for which exact analytic results have been obtained as a function of Δ. There have been recent numerical calculations of the polarizability tensor for other objects in relation to Rayleigh scattering (e.g., radar) applications [30,31]. The situation is better for limiting values of the relative conductivity Δ where the polarizability tensor $\alpha(\Delta)$ simplifies. For highly conducting inclusions, the polarizability tensor reduces to the electric polarizability α_e,

$$\lim_{\Delta\to\infty}\alpha(\Delta)\equiv\alpha_e, \tag{2.3a}$$

and $[\sigma]$ for randomly oriented inclusions, having a much higher conductivity than the matrix, then equals

$$[\sigma(\Delta\to\infty)]\equiv[\sigma]_\infty=\langle\alpha_e\rangle/V_p. \tag{2.3b}$$

As above, $\langle\alpha_e\rangle$ denotes the average electric polarizability tensor. The case of insulating inclusions in a conducting medium corresponds formally to $\Delta\to 0^+$, so that we similarly have

$$\lim_{\Delta\to 0^+}\alpha(\Delta)\equiv\alpha_m, \tag{2.4a}$$

$$[\sigma(\Delta\to 0)]\equiv[\sigma]_0=\langle\alpha_m\rangle/V_p, \tag{2.4b}$$

where α_m is the magnetic polarizability (see Ref. [1] for a discussion of the magnetic-electric polarizability analogy). In the $\Delta\to 0^+$ and $\Delta\to\infty$ limits, $[\sigma]$ is simply a functional of particle shape and spatial dimension. In our previous paper

we discussed the important exact relation of α_m to the hydrodynamic virtual mass of the particle, which yielded many exact results for this quantity [1].

The intrinsic conductivity is rather insensitive to particle shape when the conductivity of the particles is similar to the embedding medium ($\Delta \approx 1$), and a formal Taylor expansion about this limit can be made. Explicit calculation shows that this expansion does not depend on particle shape at all to second order in $(\Delta-1)$ [32,33],

$$[\sigma(\Delta)]=(\Delta-1)+[\sigma'']\Delta-1)^2+O((\Delta-1)^3), \quad (2.5)$$

$$[\sigma'']\equiv\frac{1}{2}\frac{\partial^2[\sigma(\Delta)]}{\partial\Delta^2}\bigg|_{\Delta=1},$$

where $[\sigma'']=-1/d$ [28] for the electrical problem in d dimensions. Equation (2.5) is found to be very useful in Sec. III, where an approximant for $[\sigma(\Delta)]$ is developed for particles of general shape.

More general results are possible for $[\sigma(\Delta)]$ in the superconducting and insulating particle limits in $d=2$ based on general conformal mapping results. In particular, the intrinsic conductivity of an arbitrarily shaped superconducting inclusion $[\sigma]_\infty$ can be exactly expressed [1] in terms of the ''transfinite diameter'' C_L of the inclusion [34,35] (see below)

$$[\sigma]_\infty=2A_c/A, \quad A_C=\pi C_L^2, \quad (2.6)$$

where A is the area of the inclusion. Moreover, the Keller-Mendelson inversion theorem [36] for $d=2$ implies that $[\sigma]$ for an insulating inclusion, $[\sigma]_0$, is related to $[\sigma]_\infty$ by a change of sign,

$$[\sigma]_0=-[\sigma]_\infty, \quad d=2. \quad (2.7)$$

The transfinite diameter C_L is a basic measure of the average size of a bounded plane set, and can be defined in a variety of equivalent ways [35,37]. C_L, for example, is defined as the conformally invariant magnitude of Dirichlet's integral associated with the exterior of the region defining the particle [35]. The equivalent transfinite diameter can be expressed in terms of the Euclidean metric defining the distance between points in the set [37]. Perhaps the most useful definition of C_L involves the purely geometrical construction of mapping the exterior of a region Σ having an arbitrary but simply connected shape and finite area onto a circular region in such a fashion that the points at a large distance from Σ are asymptotically unaffected by the transformation [38]. The radius of this uniquely defined transformed circular region equals C_L. This transformation is basically the content of the Riemann mapping theorem [39]. Since C_L is a central object of harmonic analysis in two dimensions, there exist extensive tabulations of C_L [34,35]. We may combine this information with (2.6) and (2.7) to obtain *exact* results for $[\sigma]_0$ and $[\sigma]_\infty$ in $d=2$. An extensive tabulation of exact analytic results for symmetrically shaped regions and numerical estimates of these virials for irregularly shaped regions have been given in our previous paper for $d=2$ and also for $d=3$ [1].

Unfortunately, real inclusions often do not correspond to the ideal limits of perfectly insulating $(\Delta=0)$ and perfectly conducting $(\Delta\to\infty)$ inclusions, and explicit calculation (see Sec. III) shows that the extent to which these limits apply depends on particle asymmetry. There is a need for accurate estimates of $[\sigma(\Delta)]$ for variable Δ if accurate inference of particle shape from conductivity (or other related property) measurements is required.

Exact results for general values of Δ are very limited, however. Maxwell's [3] and Sangani's [4] result for spheres were mentioned in Eq. (2.1). The ellipsoid in $d=3$ is also analytically tractable, although no simple closed form analytic expression exists for $[\sigma(\Delta)]$, even for this simple class of particle shapes (except for ellipsoids of revolution [1]). The final known $[\sigma(\Delta)]$ expression is for an elliptical inclusion in $d=2$,

$$[\sigma(\Delta)]=\frac{(\Delta^2-1)(1+x)^2}{2(1+\Delta x)(\Delta+x)}, \quad (2.8)$$

where x is the ratio of the semimajor to semiminor axis lengths. In Sec. III we provide an approximant for $[\sigma]$ for particles of general shape based on previously tabulated values of $[\sigma]_0$ and $[\sigma]_\infty$ [1], the spatial dimension d, and Δ.

III. INTRINSIC CONDUCTIVITY FOR GENERAL Δ

The limiting values of $[\sigma]$ for $\Delta\to\infty$ and $\Delta\to0$ and the expansion of $[\sigma(\Delta)]$ to second order in $(\Delta-1)$ provides five pieces of information about $[\sigma(\Delta)]$ corresponding to bodies of general shape. Explicit numerical and analytical calculations (see below) of $[\sigma(\Delta)]$ indicate that this function always seems to increase monotonically with Δ. Based on these results, we introduce a Padé approximant [41] to describe $[\sigma(\Delta)]$ for general shaped bodies and values of Δ,

$$[\sigma(\Delta)]=\frac{[\sigma]_\infty(\Delta-1)^2+a(\Delta-1)}{(\Delta-1)^2+([\sigma]_\infty-a[\sigma''])(\Delta-1)+a}. \quad (3.1a)$$

$$a\equiv\frac{[\sigma]_\infty-[\sigma]_0+[\sigma]_\infty[\sigma]_0}{1+(1+[\sigma''])[\sigma]_0} \quad (3.1b)$$

Equation (3.1a) was constructed by starting with a ratio of two quadratic polynomials in Δ. This ratio has five independent coefficients. These five coefficients are then determined from the five pieces of information mentioned above: the value of $[\sigma(\Delta)]$ and its first two derivatives at $\Delta=1$, and the values of $[\sigma]_0$ and $[\sigma]_\infty$. An approximation with a similar mathematical form was introduced previously by Eyges and Gianino [42] to summarize their numerical results for the polarizability of a cube $(d=3)$ as a function of the relative dielectric constant of the cube to the surrounding medium (see below). We also observe that Eq. (3.1) in $d=2$ reduces to the exact result for an ellipse, Eq. (2.8). The $\Delta\to\infty$ limit for an ellipse is given by

$$[\sigma]_\infty=(1+x)^2/(2x). \quad (3.2)$$

Eq. (3.1) also recovers $[\sigma(\Delta)]$ for hyperspheres in d dimensions given in (2.1b). It is a good test of our approximate formula that it reduces to the exact equations in known limits.

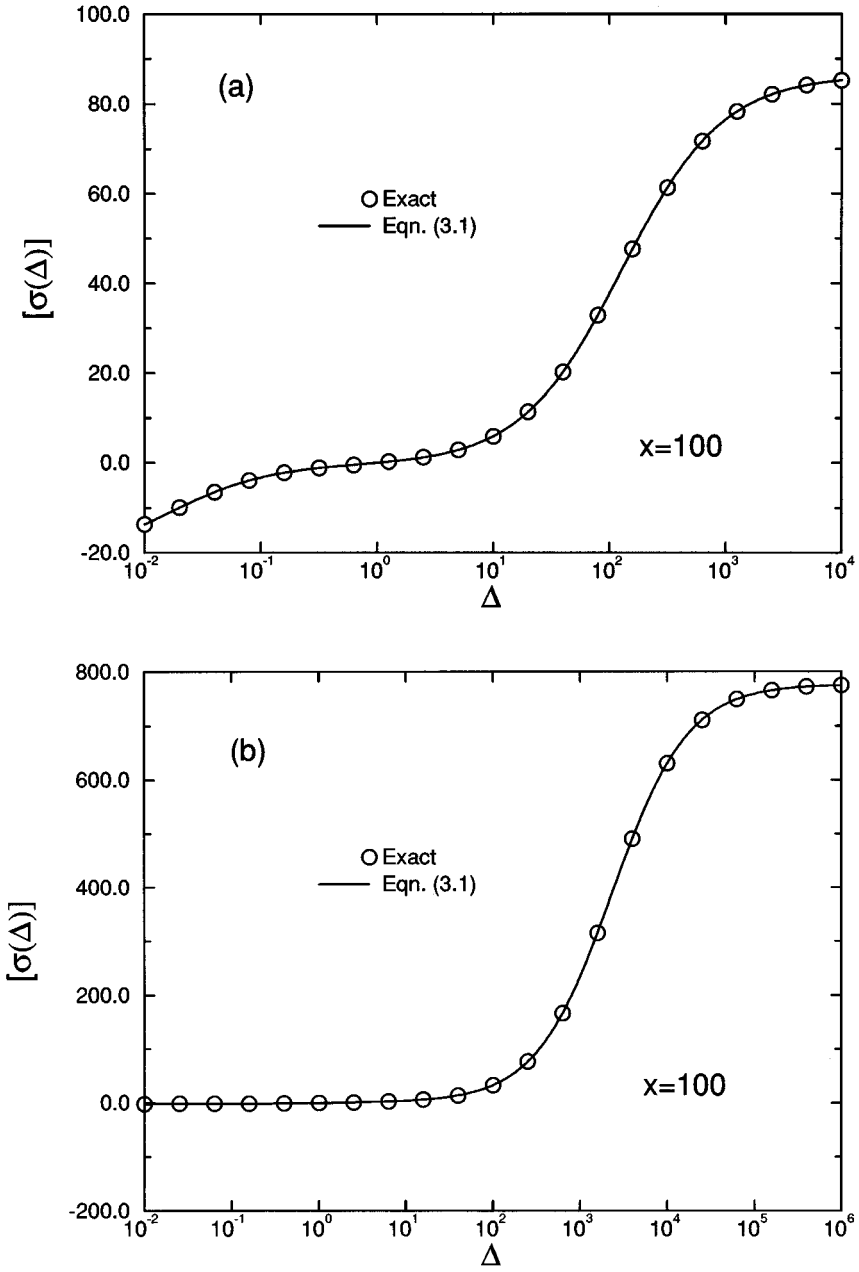

FIG. 1. The intrinsic conductivity $[\sigma(\Delta)]$ vs the relative conductivity Δ for an (a) oblate and a (b) prolate ellipsoid of revolution, with the ratio of the longest axis to the shortest axis equal to 100. The solid line is the Padé approximant Eq. (3.1), and the circles are the exact result for a selected number of values of Δ.

As a further test of Eq. (3.1), we consider $[\sigma(\Delta)]$ for ellipsoids of revolution where exact analytical results are known. In Figs. 1(a) and 1(b), we compare the exact results for $[\sigma(\Delta)]$ to the approximant Eq. (3.1) for oblate and prolate ellipsoids of revolution where the ratio of the larger to the smaller axis lengths in each case equals 100. Each example reveals a nontrivial variation of $[\sigma]$ with Δ, which is accurately described by the approximant (3.1). Deviations were less than 0.2% for the prolate case, and were exact within computer roundoff error (ten significant digits) for the oblate case.

Some further insight into these crossover curves for $[\sigma(\Delta)]$ at high aspect ratios can be obtained from the exact $d=2$ ellipse result. Figure 2 shows this function covering six orders of magnitude in the aspect ratio x. The inflection points in Fig. 2 scale linearly with x on the $\log_{10}\Delta$ scale (there are no inflection points on a regular Δ scale). Evidently, Δ must be increasingly large or small as the aspect ratio of the particles increases for these particle shapes to correspond to the limiting superconducting or insulating particle limits.

We next consider some finite element calculations of $[\sigma(\Delta)]$ that generalize our previous calculations for insulating and highly conducting particles [1]. In these calculations particles are represented as digital images built up from cubical elements. A standard lattice of size 120^3 was used, which is the largest that was practical considering both computer memory and running time. Because of the overall computational cell size limit, a compromise had to be taken between using enough pixels to give a good representation of the particle, and keeping the particle small compared to the overall unit cell, so as to keep the volume fraction small enough to be in the linear regime in concentration. The size and complexity of the objects that could be treated in this fashion is necessarily limited, but a good approximation to a wide range of physically interesting objects could still be

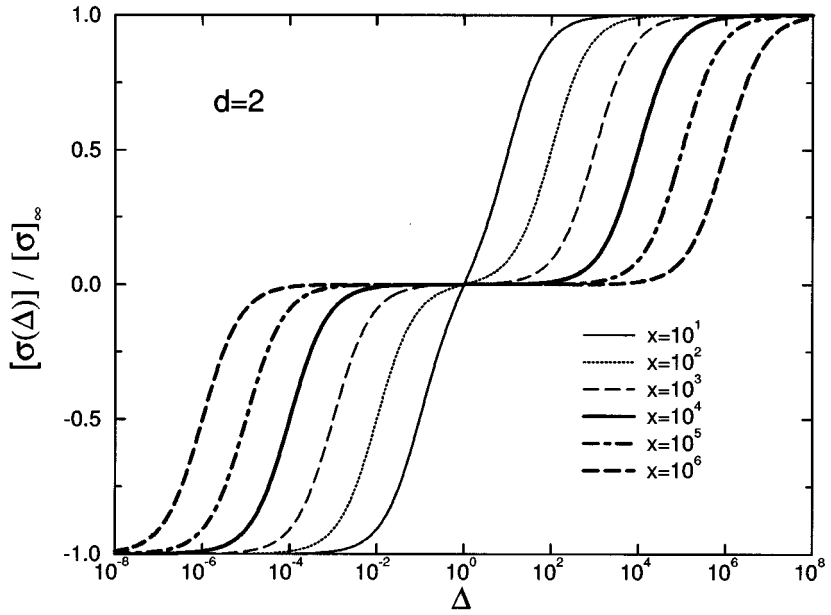

FIG. 2. The intrinsic conductivity $[\sigma(\Delta)]$ divided by the superconducting limit $[\sigma]_\infty$ vs the relative conductivity Δ for a series of $d=2$ ellipses with varying aspect ratio x.

obtained. The typical computational time for about 20 values of Δ and a particular shape was about 10 h on a Convex 3820 supercomputer. Details of our computational procedure were given in our previous paper [1]. Comparisons of these calculations against exactly soluble examples showed a systematic overestimation of $[\sigma]_\infty$ of about 5–6 % in $d=3$, for higher values of Δ, and a smaller underestimation, of 2–3 %, in $d=2$ [1].

Figure 3 shows the important case of a cube as a function of Δ where the solid line denotes the approximant Eq. (3.1) using the numerical estimates of Eyges and Gianino [42],

$$[\sigma]_0=-1.59, \quad [\sigma]_\infty=3.40. \tag{3.3}$$

The results in Fig. 3 agree with the numerical results of Eyges and Gianino [42] to within 1%, and usually the agreement is much better. Eyges and Gianino evaluated $[\sigma(\Delta)]$ based on a numerical solution of an integral equation describing this problem.

Finite element calculations were performed for rectangular parallelipipeds having dimension ratios 2:2:1 and 1:1:2. Equation (3.1) again gives an excellent description, and thus we only summarize the limiting values of $[\sigma]$ needed to reproduce these results:

$$[\sigma(2{:}2{:}1)]_0=-1.68, \quad [\sigma(2{:}2{:}1)]_\infty=4.15, \tag{3.4a}$$

$$[\sigma(1{:}1{:}2)]_0=-1.65, \quad [\sigma(1{:}1{:}2)]_\infty=4.22. \tag{3.4b}$$

We emphasize that these are finite element estimates of the intrinsic conductivity rather than the exact values.

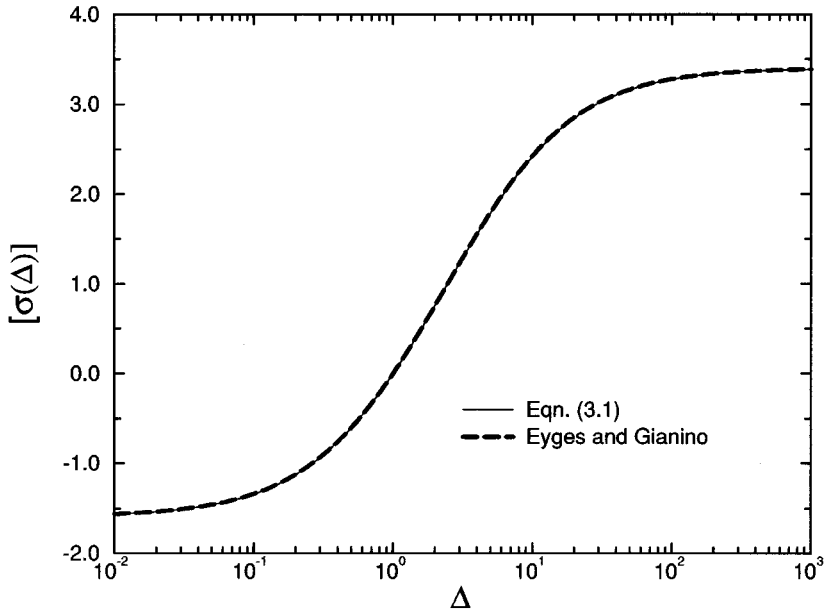

FIG. 3. The intrinsic conductivity $[\sigma(\Delta)]$ vs the relative conductivity Δ for a cube, as computed by Eyges and Gianino [42], and the Padé approximant of the text.

TABLE I. Limiting intrinsic conductivities for circular cylinders.

Diameter×height	Exact $[\sigma]_\infty$	Numerical $[\sigma]_\infty$	Numerical $[\sigma]_0$
$1\times\frac{1}{2}$	4.106	4.32	−1.60
1×1	3.401	3.56	−1.57
1×2	3.622	3.79	−1.64
1×4	4.704	4.93	−1.86

The important physical example of a right circular cylinder is considered next. Precise analytical calculations of the polarizability in the superconducting particle limit have been made [43], and $[\sigma]_\infty$ values based on these calculations are given in Table I. In addition, $[\sigma]_0$ has been calculated using finite element methods, and these results are also given in Table I. This comparison shows a 5–6 % error in our numerical calculations for the superconducting limit. The error for the insulating limit, while we have no exact values against which to compare them, is probably in the range of 2–3 %, based on experience with other shapes [1]. We have found that the insulating limit is usually computed more accurately with our finite element method than is the superconducting limit. Better accuracy is possible, of course, if sufficient computer memory is available, at the expense of much greater computational times. Accurate numerical data for $[\sigma]_\infty$ and $[\sigma]_0$, for a wide range of diameter-height ratios, could be used to obtain approximants for these virials that then could be used in conjunction with Eq. (3.1) to make more general analytical estimates of $[\sigma(\Delta)]$ for comparison with experiments on cylindrical conducting fibers.

In our next example we treat an idealized ''spongelike'' body. Consider a cube of unit edge length, in which a square

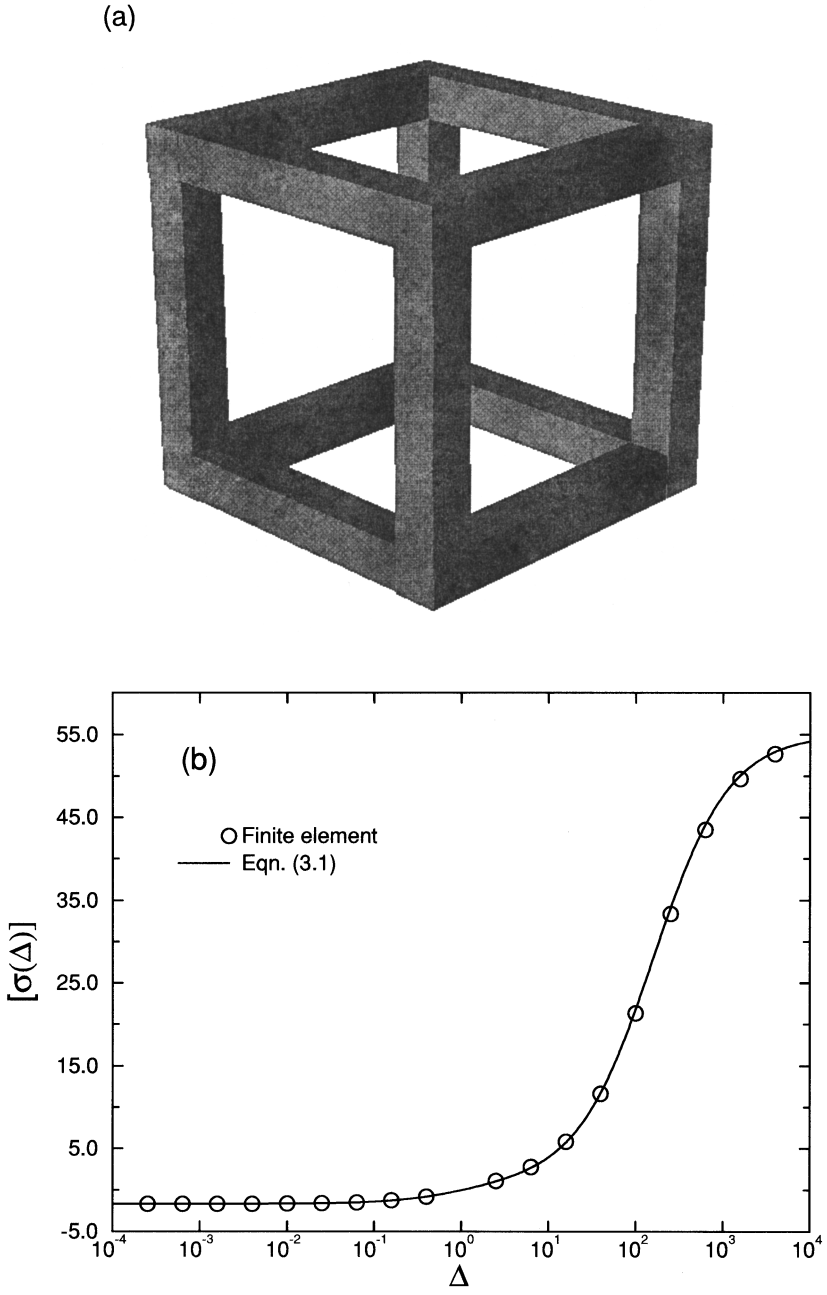

FIG. 4. (a) Image of a ''sponge.'' (b) The intrinsic conductivity $[\sigma(\Delta)]$ vs the relative conductivity Δ for the sponge model for $m=23/27$. The solid line is the Padé approximant, and the circles are the result of finite element calculations for a selected number of values of Δ.

TABLE II. Numerical estimates of intrinsic conductivity for various shapes ($d=3$).

Shape	m	$[\sigma]_\infty$	$[\sigma]_0$
Sponge	15/27	8.74	-1.75
Sponge	21/27	27.1	-1.72
Sponge	23/27	55.0	-1.66
Sponge	25/27	192	-1.43
Sponge	33/35	311	-1.43
Jack [a]		4.50	-1.51
Ring [a]		127	-1.42
Hollow tube [a]		16.7	-4.27

[a]See Ref. [1] for the dimensions of these structures.

channel is cut through the center of each face, where each channel passes completely through the cube. A picture of an object of this kind is shown in Fig. 4(a). The parameter m is taken to be the edge length of the cutout face in units of the total cube edge length. We obtain a rigid cubic wire frame when m approaches 1. Notice that cutting out the center, which makes the particle more spongelike, has a very large effect on $[\sigma]_\infty$, as can be seen in Table II. It would be interesting to push the effect to the extreme in a different way by generating a Menger sponge [44] fractal by a repeated decimation of the cube at different scales, so that $[\sigma]_\infty$ would diverge in a fashion related to the fractal dimension of the sponge. The memory capacity of our computer was not large enough to allow us to consider more than one or two generations of such an iteratively constructed ''diffuse'' object, so we presently confine ourselves to the first generation wire frame structure shown in Fig. 4(a).

Figure 4(b) presents our numerical results as a function of Δ for the sponge with $m=23/27$. Note that $[\sigma(\Delta)]$ is quite insensitive to Δ for relatively insulating particles ($\Delta<1$), which is typical for extended or diffuse objects. As in previous comparisons, the approximant Eq. (3.1) describes the numerical data very well. Table II includes numerical data for $[\sigma]_0$ corresponding to other representative shapes considered in our previous paper [1]. A ''jack'' is a sphere punctured by three intersecting rectangular parallelipipeds. The square ring and square hollow tube are self-explanatory. Values of $[\sigma]_0$ were not given in our previous paper, which focused on comparisons between $[\sigma]_\infty$ and the intrinsic viscosity $[\eta]$.

Numerical calculations of $[\sigma(\Delta)]$ for inclusions having sharp corners give rise to subtle variations of this virial coefficient with Δ. Such cases provide a good test for our approximant Eq. (3.1). In Fig. 5 we consider finite element calculations for a 12:1 rectangular region in $d=2$ (the lattice size in $d=2$ was 1800^2). Observe the subtle feature of a ''wavy'' variation of $[\sigma(\Delta)]$ for this type of inclusion, which is followed by Eq. (3.1) remarkably well. In the insulating limit, we found

$$[\sigma(12:1)]_0=-6.29=-[\sigma(12:1)]_\infty . \tag{3.5}$$

The exact value of $[\sigma]_0$ for a 12:1 rectangle is -6.38 [40], indicating an error of only 1.4% for the finite element method at this resolution in $d=2$. The values of $[\sigma]$ for finite Δ should have even less error. To save computer time, in all the $d=2$ finite element computations we took advantage of the Keller-Mendelson inversion theorem [36] and only calculated $[\sigma(\Delta)]$ for $\Delta<1$.

As a final example, we considered a completely asymmetric inclusion to make sure that particle asymmetry did not invalidate our approximant. Two dimensions was chosen to allow a higher resolution to be used in order to obtain more accurate computational results. The L-shaped asymmetric particle, of no particular symmetry, chosen to illustrate this case is shown in the inset of Fig. 6. Equation (3.1) again provides a very good approximation of the intrinsic conductivity data (Fig. 6), where we found

$$[\sigma(L)]_0=-3.11=-[\sigma(L)]_\infty . \tag{3.6}$$

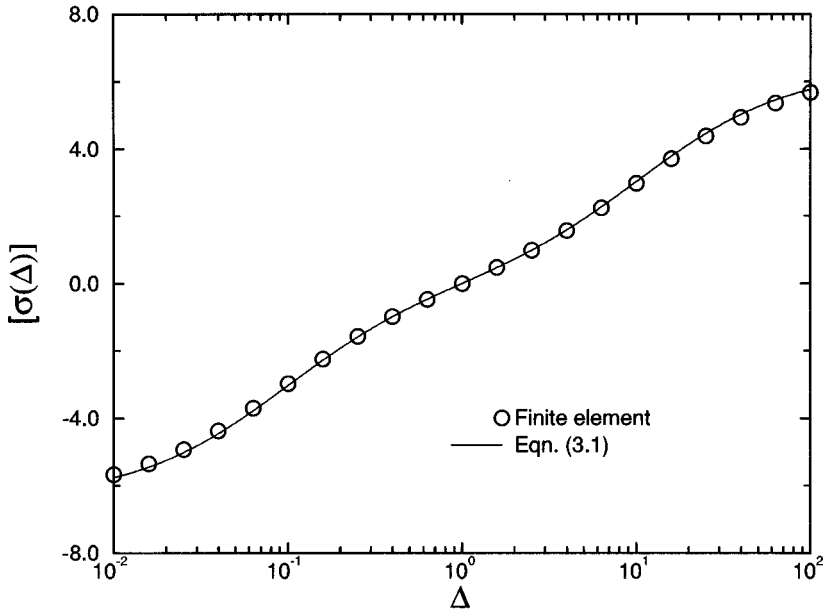

FIG. 5. The intrinsic conductivity $[\sigma(\Delta)]$ vs the relative conductivity Δ for 1×12 rectangular region in $d=2$. The solid line is the Padé approximant, and the circles are the result of finite element calculations for a selected number of values of Δ.

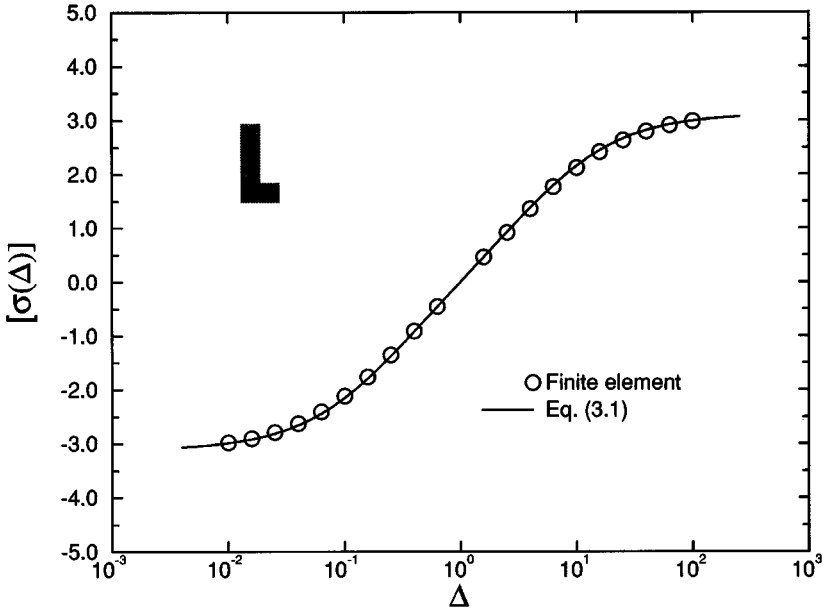

FIG. 6. The intrinsic conductivity $[\sigma(\Delta)]$ vs the relative conductivity Δ for a $1\times2\times4$ L-shaped region in $d=2$. The solid line is the Padé approximant, and the circles are the result of finite element calculations for a selected number of values of Δ.

This agreement for many different kinds of particles, including a completely anisotropic one, suggests that Eq. (3.1) should be a very reasonable approximation for a wide range of complex-shaped particles.

IV. DISCUSSION

The problem of calculating the effective properties of a medium containing dispersed particles having complex shape and different properties than the suspending matrix arises in many applications. For many properties (refractive index, dielectric constant, magnetic permeability, thermal and electrical conductivity, tracer diffusion constant) this general problem reduces to a common mathematical description [1,27–29]. In the present paper we have specialized the language to electrical conductivity to make our discussion more concrete. We have also confined our attention to the dilute regime where each inclusion independently influences the properties of the medium, and where exact calculations for special shapes become possible, at least for limiting values of the relative conductivity Δ and specially shaped inclusions.

The computationally more difficult and practically important problem of the conductivity virial coefficient $[\sigma(\Delta)]$ for arbitrary Δ has been attacked by the pragmatic procedure of developing an approximant incorporating exact information for $\Delta\approx1$ and numerical (and sometimes exact analytical) information for $[\sigma(\Delta)]$ in the insulating ($\Delta\to0$) and superconducting ($\Delta\to\infty$) limits. Numerical calculations of $[\sigma(\Delta)]$ for particles having a variety of shapes have shown very good agreement with this approximant. However, the utilization of Eq. (3.1) for estimating $[\sigma(\Delta)]$ for generally shaped particles in $d=3$ is still limited by the difficulty in calculating the virial coefficients in these limits.

Given these difficulties, it is useful to also develop some simple approximations for $[\sigma]_0$ and $[\sigma]_\infty$ appropriate for commonly encountered classes of inclusions. In Fig. 7 we give exact results for $[\sigma]_0$ and $[\sigma]_\infty$ for an ellipsoid of revolution as a function of the aspect ratio x (dimension of ellipsoid along axis of symmetry relative to dimension normal to axis of symmetry). This figure shows that for needlelike particles $[\sigma]_0$ is insensitive to particle shape. For a sphere, $[\sigma]_0=-\frac{3}{2}$, and for an infinitely thin needle $[\sigma]_0=-\frac{5}{3}$, so we expect that the average of these results,

$$[\sigma]_0\approx-\tfrac{19}{12}\pm0.15, \tag{4.1}$$

should be a useful approximation for insulating particles modestly extended along one direction. Equation (4.1) should perhaps also apply to diffuse spongelike structures, as in Fig. 4, and to random-coil polymers, which have a low density. A similar approximation is often employed in aerodynamic literature for the virtual mass of an object [45], which is directly related to $[\sigma]_0$ [1]. The approximation Eq. (4.1) is poor for sheetlike insulating structures, which strongly modify the conductivity of a conducting matrix (see Fig. 7), so the approximation should not be employed uncritically.

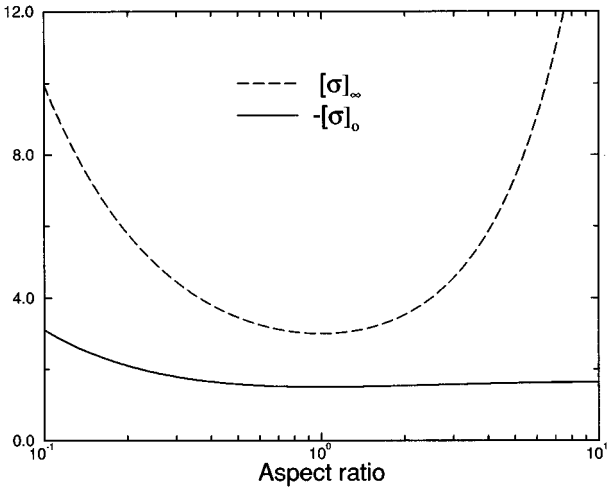

FIG. 7. Intrinsic conductivities $[\sigma]_0$ and $[\sigma]_\infty$ for ellipsoids of revolution as a function of aspect ratio x.

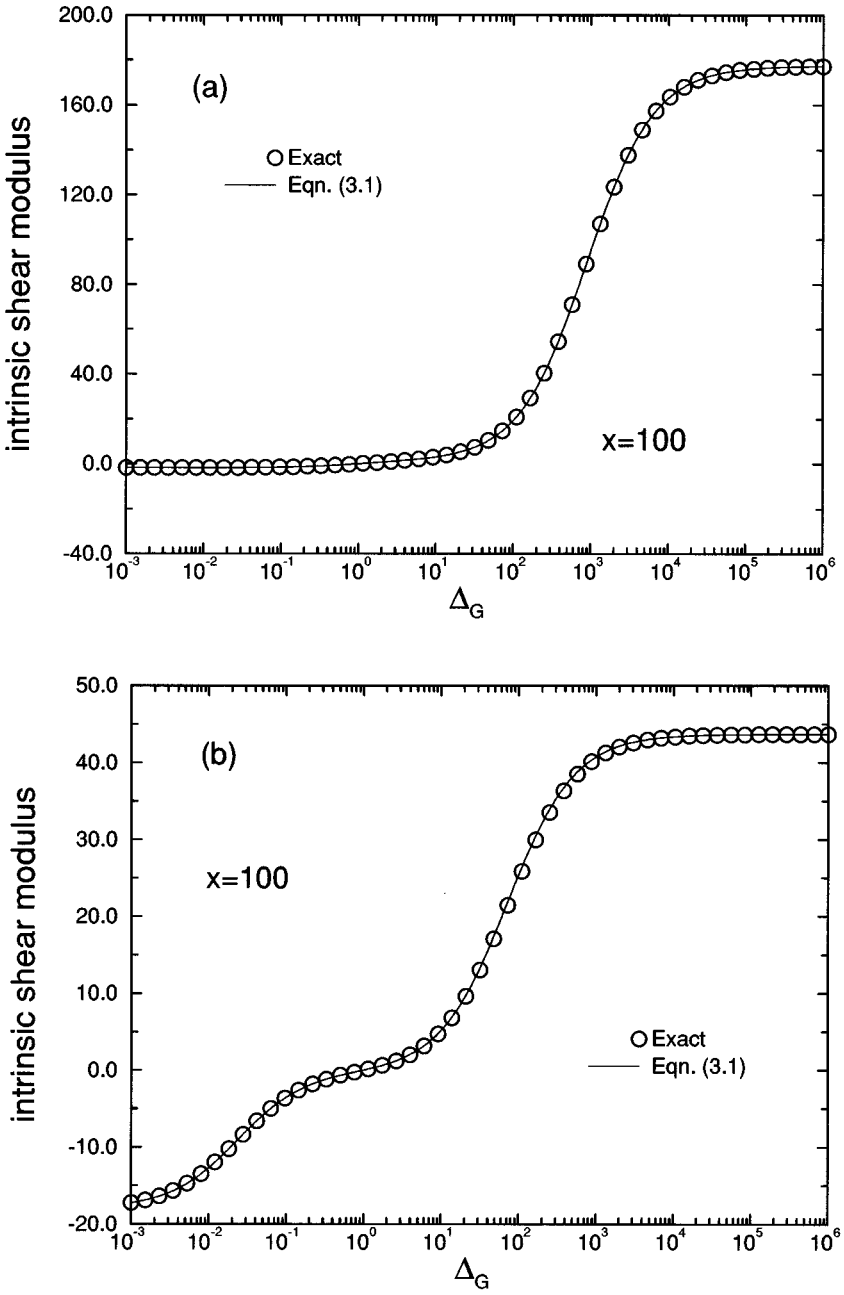

FIG. 8. The intrinsic shear modulus $[G(\Delta)]$ vs the relative shear modulus Δ_G for (a) a prolate and (b) an oblate ellipsoid of revolution, with the ratio of the longest axis to the shortest axis equal to 100. The solid line is the Padé approximant Eq. (3.1), and the circles are the exact result for a selected number of values of Δ.

There are actually few previous calculations of $[\sigma]_0$ for any shape, so some comment on other applications of this shape functional are worth mentioning. Wang [46] (with Onsager's advice) investigated the role of protein particle shape on the self-diffusion coefficient D_s of water in protein solutions, and found the concentration dependence

$$D_s/D_s(\phi\rightarrow 0)=1+[\sigma]_0\phi+O(\phi^2), \tag{4.2}$$

where ϕ is the protein volume fraction. The notation of the present paper is adopted in Eq. (4.2) (see also Appendix A of Ref. [1] for further discussion). Recent NMR measurements on the diffusion of water in swollen gels by Geissler and Hecht [47] have shown that $[\sigma]_0\approx -1.66$, which is the expected result for slender particles [see Eq. (4.1) and Fig. 7]. Wang discusses the importance of virial expansions such as Eq. (4.2) for inferring the particle shape and surface properties of suspended particles [46], and there are also many classic polymer science studies devoted to this general problem [48].

The $[\sigma]_\infty$ virial exhibits a more complex shape dependence. In our previous paper we established a general approximate relation between $[\sigma]_\infty$ and the intrinsic viscosity $[\eta]$ of a suspension of rigid particles, $[\eta]\approx[(d+2)/2d][\sigma]_\infty$. A slender body approximation of Debye [49] for $[\eta]$, and an approximation relating the translational friction f_T of a Brownian particle to the capacity of the particle C [50] (Newtonian capacity C rather than the logarithmic capacity C_L discussed above), suggests a general approximation for $[\sigma]_\infty$ corresponding to linearly extended particles such as polymer chains, needlelike inclusions, etc.:

$$[\sigma]_\infty\approx(6\pi/5)R_g^2C/V_p, \tag{4.3}$$

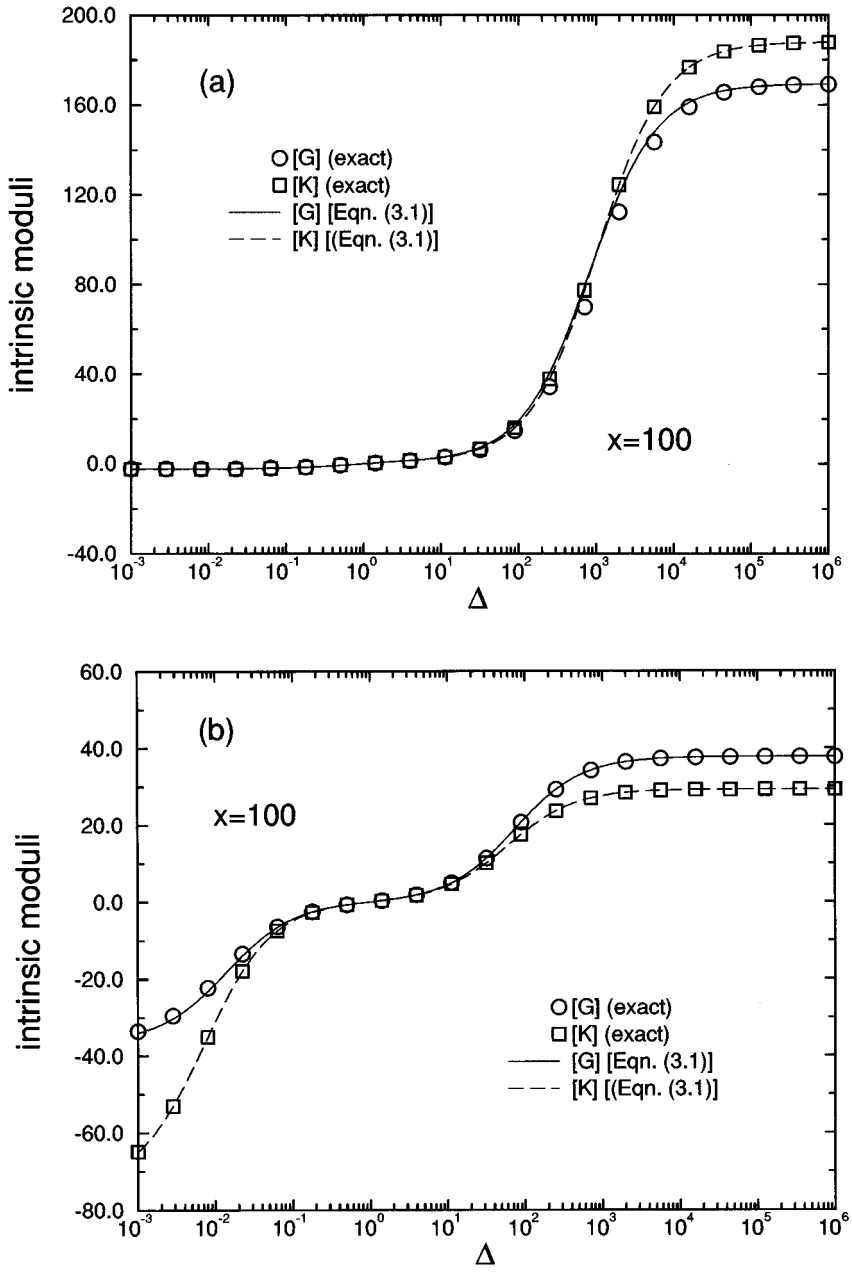

FIG. 9. The intrinsic bulk and shear moduli $[K(\Delta)]$ and $[G(\Delta)]$, vs the relative bulk and shear moduli $\Delta=\Delta_K=\Delta_G$ for (a) a prolate and (b) an oblate ellipsoid of revolution ($d=3$), with the ratio of the longest axis to the shortest axis equal to 100. The solid line is the Padé approximant Eq. (3.1), and circles are the exact result for a selected number of values of Δ. The matrix Poisson's ratio $\nu_0=5/22$.

where R_g is the average particle radius of gyration and V_p is the particle volume. The scaling $[\sigma]_\infty \sim R_g^2 C/V_p$ is consistent with exact calculations for long ellipsoidal particles where $[\sigma]_\infty$ scales with aspect ratio x as [1,51]

$$[\sigma]_\infty \sim (x^2/3)/\ln(x). \tag{4.4}$$

Equation (4.3) is potentially a useful approximation since R_g is readily calculated from simple geometry, and accurate and efficient numerical methods have recently been developed for calculating C of general shaped objects [49,52]. Future numerical work should examine the ratio Γ,

$$\Gamma = \frac{R_g^2 C}{[\sigma]_\infty V_p}, \tag{4.5}$$

to determine the degree of its universality, at least for bodies extended along one direction. The development of readily implemented and accurate approximations for $[\sigma]_0$ and $[\sigma]_\infty$ should be very useful in estimating $[\sigma(\Delta)]$ of polymeric particles. For example, the relation Eq. (4.3) implies a nontrivial molecular weight dependence of $[\sigma]$ for suspensions of highly conducting polymers [1], and a correspondingly strong influence on the conductive properties of solutions of these polymers.

The problem of calculating transport virial coefficients as a function of the relative property Δ is commonly encountered. The treatment of the conductivity σ applies equally as well to thermal conductivity, dielectric constant, refractive index, magnetic permeability, and other properties [27–29]. There are also many applications involving the elastic constants of solid composites and the viscosity of suspensions that involve similar, but somewhat more complicated mathematics. For example, the virial coefficient $[G]$ for the shear modulus of an elastic particle in an incompressible medium

depends on the ratio Δ_G of the shear modulus of the particle to that of the embedding medium and the intrinsic shear viscosity $[\eta]$ of a suspension of fluid particles depends on the relative viscosity Δ_η [1]. These virials can also depend on the surface boundary condition (partial slip) and on other parameters (Poisson ratio, surface shear viscosity, or modulus, etc.) in addition to a general dependence on particle shape. It turns out to be possible to treat this general class of problems by basically the same Padé approximant method.

To illustrate this generality, we also consider the calculation of the intrinsic shear modulus $[G]$. For this generalization we simply replace σ by G in Eq. (2.5) and note the corresponding result for $[G'']$ in $d=2$ and $d=3$,

$$[G'']=-2/(d+2), \tag{4.6}$$

which can be inferred from Refs. [29,53,54]. In Figs. 8(a) and 8(b) we compare exact results [55] to the approximant Eq. (3.1) with G replacing σ for randomly oriented prolate and oblate ellipsoids of revolution with relative shear modulus Δ_G. As in the conductivity virial case, the agreement is excellent. The calculation of the intrinsic viscosity $[\eta]$ is very similar to the calculation of $[G]$ [1,56], so it should be possible to extend Eq. (3.1) to these properties as well.

For the general elastic case, when particles with bulk and shear moduli K_p and G_p are embedded in a matrix with K_0 and G_0 ($\Delta_K=K_p/K_0$ and $\Delta_G=G_p/G_0$), the same Padé approximant again holds. The quantities $[G'']$ and $[K'']$ are given, in $d=3$, by

$$[G'']=\frac{-2(4-5\nu_0)}{15(1-\nu_0)}, \tag{4.7}$$

$$[K'']=\frac{-(1+\nu_0)}{3(1-\nu_0)}, \tag{4.8}$$

and in $d=2$ by

$$[G'']=-\frac{1}{4}(3-\nu_0) \tag{4.9}$$

$$[K'']=-\frac{1}{2}(1+\nu_0), \tag{4.10}$$

where ν_0 is the Poisson's ratio of the matrix [54]. In the small (Δ_K-1) and (Δ_G-1) limits, the expansion for K depends only on (Δ_K-1) and that for G only on (Δ_G-1), to second order in these quantities [54]. These quantities can also be obtained from the Hashin elastic bounds [29,53] for the moduli, which are known to be exact to second order in (Δ_K-1) and (Δ_G-1). Using the exact solution for $[G]$ and $[K]$ for ellipsoids of revolution ($d=3$) [55], Eq. (3.1) again agrees very well for randomly oriented prolate and oblate ellipsoids of revolution, as can be seen in Figs. 9(a) and 9(b). Having worked well for both electric and elastic cases, for a wide variety of particle shapes, we then expect the Padé approximant may apply to other properties as well.

[1] J. F. Douglas and E. J. Garboczi, Adv. Chem. Phys. **91**, 85 (1995). See extensive list of references therein to effective property calculations.

[2] H. Yamakawa, *Modern Theory of Polymer Solutions* (Harper and Row, New York, 1971); J. F. Douglas, J. Roovers, and K. F. Freed, Macromolecules **23**, 4168 (1990).

[3] J. C. Maxwell, *A Treatise on Electricity and Magnetism* (Dover, New York, 1954).

[4] D. J. Bergman, Phys. Rep. **9**, 377 (1978).

[5] A. S. Sangani, Soc. Ind. Appl. Math. J. Appl. Math. **50**, 64 (1990).

[6] H. B. Levine and D. A. McQuarrie, J. Chem. Phys. **49**, 4181 (1968).

[7] D. J. Jeffrey, Proc. R. Soc. London Ser. A **335**, 355 (1973).

[8] A. Voet, J. Phys. Chem. **51**, 1037 (1947).

[9] C. Pearce, Brit. J. Appl. Phys. **6**, 113 (1955); R. Guillien, Ann. Phys. (Paris) **16**, 205 (1941).

[10] R. E. De La Rue and C. W. Tobias, J. Electrochem. Soc. **106**, 827 (1959).

[11] L. Sigrist and O. Dossenbach, J. Appl. Electrochem. **10**, 223 (1980).

[12] C. R. Turner, Chem. Eng. Sci. **31**, 487 (1976).

[13] H. Fricke, Phys. Rev. **24**, 575 (1924); H. Fricke and S. Morse *ibid.* **25**, 361 (1925).

[14] C. J. Bottcher, *Theory of Electric Polarization* (Elsevier, Amsterdam, 1952).

[15] D. Polder and J. H. Van Santen, Physica **12**, 27 (1946); N. Hill, W. E. Vaugh, A. H. Price, and M. Davis, *Dielectric Properties and Molecular Behavior* (Van Nostrand Reinhold, New York, 1969); A. Lakhtakia, Chem. Phys. Lett. **174**, 583 (1990).

[16] J. B. Keller, Philips Res. Rep. **30**, 83 (1975).

[17] J. B. Keller, R. E. Kleinman, and T. B. A. Senior, J. Inst. Math. Appl. **9**, 14 (1972); D. S. Jones, *ibid.* **23**, 421 (1979); G. Birkhoff, in *Studies in Mathematics and Mechanics: Essays in Honor of Richard Von Mises* (Academic, New York, 1954), pp. 88-96.

[18] S. Szegö, Duke Math. J. **16**, 209 (1949).

[19] M. Schiffer and G. Szegö, Trans. Am. Math. Soc. **67**, 130 (1949).

[20] A. Rocha and A. Acrivos, Quart. J. Mech. Appl. Math **26**, 217 (1973); H.-S. Chen and A. Acrivos, Proc. R. Soc. London **349**, 261 (1976).

[21] W. E. Kock, Bell. Syst. Tech. J. **27**, 58 (1948).

[22] G. Estrin, J. Appl. Phys. **21**, 667 (1950).

[23] S. Cohn, J. Appl. Phys. **20**, 257 (1949); **22**, 628 (1951).

[24] R. E. Collin, *Field Theory of Guided Waves* (McGraw-Hill, New York, 1960).

[25] P. Debye, J. Appl. Phys. **15**, 338 (1944); A. Peterlin, in *Rheology*, edited by F. R. Eirich (Academic, New York, 1956), Vol. 1.

[26] J. Stratton, *Electromagnetic Theory* (McGraw-Hill, New York, 1941); H. C. Chen, *Theory of Electromagnetic Waves* (McGraw-Hill, New York, 1983); G. Dassios and R. E. Klein-

man, SIAM Rev. **31**, 565 (1989); L. Eyges, Ann. Phys. **90**, 266 (1975).
[27] G. K. Batchelor, Ann. Rev. Fluid Mech. **6**, 227 (1974).
[28] S. Torquato, Appl. Mech. Rev. **44**, 37 (1991).
[29] Z. Hashin, J. Appl. Mech. **50**, 481 (1983).
[30] R. E. Kleinman and T. B. A. Senior, Radio Sci. **7**, 937 (1972); T. B. A. Senior, *ibid.* **17**, 741 (1982).
[31] K. M. Siegel, Proc. IEEE **51**, 232 (1962).
[32] W. F. Brown, J. Chem. Phys. **23**, 1514 (1955).
[33] L. D. Landau and E. M. Lifshitz, *Electrodynamics of Continuous Media* (Pergamon, New York, 1960).
[34] G. Pólya and G. Szegö, *Isoperimetric Inequalities in Mathematical Physics* (Princeton University Press, Princeton, 1951).
[35] N. S. Landkof, *Foundations of Modern Potential Theory* (Springer-Verlag, New York, 1972).
[36] J. B. Keller, J. Math. Phys. **5**, 548 (1964); K. S. Mendelson, J. Appl. Phys. **46**, 917 (1975).
[37] G. Szegö, in *Proceedings of the Conference on Differential Equations*, edited by J. B. Diaz and L. E. Payne (University of Maryland Bookstore, College Park, MD, 1956), p. 139; M. Schiffer, Proc. Cambridge Philos. Soc. **37**, 373 (1941).
[38] G. Pólya, Proc. Natl. Acad. Sci. (U.S.A.) **33**, 218 (1947).
[39] L. V. Ahlfors, *Conformal Invariants: Topics in Geometric Function Theory* (McGraw-Hill, New York, 1973).
[40] J. H. Hetherington and M. F. Thorpe, Proc. Roy. Soc. London Ser. A **438**, 591 (1992); M. F. Thorpe, *ibid.* **437**, 215 (1992).
[41] C. M. Bender and S. A. Orszag, *Advanced Mathematical Methods for Scientists and Engineers* (McGraw-Hill, New York, 1978).
[42] L. Eyges and P. Gianino, IEEE Trans. Ant. Prop. **27**, 557 (1979).
[43] T. T. Taylor, J. Research NBS **64**, 135 (1960); M. Fixman, J. Chem. Phys. **75**, 4040 (1981).
[44] B. B. Mandelbrot, *The Fractal Geometry of Nature* (Freeman, San Francisco, 1982).
[45] G. I. Taylor, Proc. Roy. Soc. London Ser. A **120**, 13 (1928); **120**, 260 (1928); E. B. Moullin, Philos. Soc. Proc. **24**, 400 (1928).
[46] J. H. Wang, J. Am. Chem. Soc. **76**, 4755 (1954); J. R. Lebenhaft and K. Kapral, J. Stat. Phys. **20**, 25 (1979); M. Fixman, J. Phys. Chem. **88**, 6472 (1984).
[47] E. Geissler and A. M. Hecht, J. Phys. Lett. (France) **40**, 173 (1979).
[48] R. Simha, J. Appl. Phys. **13**, 147 (1942); J. W. Mehl, J. L. Oncley, and R. Simha, Nature (London) **92**, 132 (1940); M. A. Lauffer, Chem. Rev. **31**, 561 (1942); J. Am. Chem. Soc. **66**, 1188 (1944); V. A. Bloomfield, Science **161**, 1212 (1968).
[49] P. Debye, J. Chem. Phys. **14**, 636 (1946).
[50] J. F. Douglas, H.-X. Zhou, and J. B. Hubbard, Phys. Rev. E **49**, 5319 (1994).
[51] E. J. Garboczi, K. A. Snyder, J. F. Douglas, and M. F. Thorpe, Phys. Rev. E **52**, 819 (1995).
[52] J. Given, J. Hubbard, and J. Douglas (unpublished).
[53] Z. Hashin, J. Mech. Phys. Solids **13**, 119 (1965).
[54] S. Torquato (unpublished).
[55] J. G. Berryman, J. Acoust. Soc. Am. **68**, 1820 (1980).
[56] W. B. Russel and P. R. Sperry, Prog. Org. Coatings **23**, 305 (1994).